

Single MHC Mutation Eliminates Enthalpy Associated with T Cell Receptor Binding

Peter J. Miller¹, Yael Pazy², Brian Conti¹, David Riddle²
Ettore Appella³ and Edward J. Collins^{1,2*}

¹*Department of Biochemistry and Biophysics, The University of North Carolina at Chapel Hill Chapel Hill, NC 27599, USA*

²*Department of Microbiology and Immunology, The University of North Carolina at Chapel Hill, Chapel Hill NC 27599, USA*

³*Laboratory of Cell Biology National Cancer Institute National Institutes of Health Bethesda, MD 20892, USA*

The keystone of the adaptive immune response is T cell receptor (TCR) recognition of peptide presented by major histocompatibility complex (pMHC) molecules. The crystal structure of AHIII TCR bound to MHC, HLA-A2, showed a large interface with an atypical binding orientation. MHC mutations in the interface of the proteins were tested for changes in TCR recognition. From the range of responses observed, three representative HLA-A2 mutants, T163A, W167A, and K66A, were selected for further study. Binding constants and co-crystal structures of the AHIII TCR and the three mutants were determined. K66 in HLA-A2 makes contacts with both peptide and TCR, and has been identified as a critical residue for recognition by numerous TCR. The K66A mutation resulted in the lowest AHIII T cell response and the lowest binding affinity, which suggests that the T cell response may correlate with affinity. Importantly, the K66A mutation does not affect the conformation of the peptide. The change in affinity appears to be due to a loss in hydrogen bonds in the interface as a result of a conformational change in the TCR complementarity-determining region 3 (CDR3) loop. Isothermal titration calorimetry confirmed the loss of hydrogen bonding by a large loss in enthalpy. Our findings are inconsistent with the notion that the CDR1 and CDR2 loops of the TCR are responsible for MHC restriction, while the CDR3 loops interact solely with the peptide. Instead, we present here an MHC mutation that does not change the conformation of the peptide, yet results in an altered conformation of a CDR3.

© 2007 Elsevier Ltd. All rights reserved.

*Corresponding author

Keywords: MHC; TCR; binding; structure; cytotoxicity

Introduction

T cells are an integral part of the ability of the adaptive immune system to recognize virtually any pathogen that might attack the host. A critical step required for T cell activation is the recognition of peptides derived from these pathogens when presented by the major histocompatibility complex protein (MHC). Recognition of foreign peptide bound to MHC is achieved through the clonotypic

T cell receptor (TCR). Upon TCR recognition of a peptide bound to MHC (pMHC), sets of T cells either kill the cell presenting the foreign peptide (cytotoxic T cells) or produce cytokines to “help” B cells and other T cells (helper T cells). The pathogens are subsequently eliminated from the host by a combination of killing infected cells to remove reservoirs of replicating pathogen, and antibody-mediated neutralization of the pathogen outside of the cell. Although TCR binding to pMHC is paramount for T cell activation, there are still many unanswered questions regarding how TCR-pMHC interactions dictate T cell responses.

Recognition of pMHC by the TCR heterodimer is accomplished using the three complementarity determining region (CDR) loops from each chain. The CDR1 and CDR2 loops are germ-line encoded within the variable gene segment of each TCR α and TCR β chain. The CDR3 loop of each chain is unique

Abbreviations used: MHC, major histocompatibility complex; TCR, T cell receptor; pMHC, peptide bound to MHC; CDR, complementarity determining region; SPR, surface plasmon resonance; ITC, isothermal titration calorimetry.

E-mail address of the corresponding author: edward_collins@med.unc.edu

and arises through V(D)J recombination.^{1,2} While recognition of the pMHC is carried out using all the CDR loops of each chain, generally, the CDR3 makes more contacts with the bound peptide than CDR1 and CDR2.³

Engagement of TCR with pMHC may result in a variety of reactions from the T cell, and the mechanisms that generate these different responses are not understood.³ The structures of TCR bound to partial agonist or antagonist pMHC complexes do not show changes in the TCR domains that would suggest a way for the TCR to propagate a qualitatively different signal to the T cell through the plasma membrane.^{4,5} It is generally accepted that there is great plasticity in the interaction between TCR and pMHC. However, as seen in a variety of TCR-pMHC co-crystal structures, the degree and location of this plasticity is not uniform. For example, the co-crystal structures of 2C-dEV8/K^b,⁶ 2C-SIYR/K^b,⁴ and KB5-C20-pKB1/K^b⁷ when compared to crystal structures of those TCRs alone show great flexibility in the CDR3 loops of the TCR. The LC13⁸ and BM3.3⁹ TCRs undergo changes in their CDR3s and in their CDR1 and CDR2 loops. Conversely, the A6-Tax/A2¹⁰ and ELS4-EPLP/B*3501¹¹ co-crystal structures exhibit conformational changes in the peptides upon TCR-pMHC binding. Finally, the crystal structures of the 1G4 TCR alone and complexed with its pMHC ligands show no significant change in either the TCR or the pMHC.¹²

Similarly, there appear to be no general thermodynamic rules that describe TCR binding to pMHC. Although surface plasmon resonance (SPR) has been used for more than a decade to examine binding of TCR to pMHC, it measures kinetic constants between TCR and pMHC, and binding *via* Scatchard analysis or mathematically using the kinetic constants. Isothermal titration calorimetry (ITC) provides a direct measure of ΔH and is hence considered a more reliable determination of thermodynamic parameters. ITC has rarely been used for TCR-pMHC studies because of the much larger amounts of protein required for the studies. Early experiments suggested that TCR-pMHC interactions seem to be governed by large enthalpically favorable and entropically unfavorable thermodynamics.^{13–16} However, more recent thermodynamic data of L13-FLR/B8,¹⁷ A6-Tax/A2,¹⁸ and 2C-QL9/L^{d19} all show entropically favorable associations.

The human MHC, HLA-A2 (A2), is the most frequent MHC found in Caucasians and African Americans.²⁰ A large panel of A2 mutants were created by Baker *et al.* and tested against a panel of T cells.²¹ Most interesting from that study, the K66A mutant was found to adversely affect recognition of 98% of the T cells examined.²¹ K66 has been shown to be a critical residue in TCR recognition of A2, regardless of the peptide presented,^{21–24} resulting in K66 to be labeled a potential “hot spot” for TCR recognition of A2. Importantly, even though K66 interacts with the peptide, the structure of Tax/A2(K66A) shows that the K66A mutation does not alter the structure of A2 or the conformation of the Tax peptide.²⁴ However,

the effect of the K66A mutation on the cognate TCR has never been determined structurally.

AHIII12.2 (AHIII) is a murine T cell clone that recognizes human HLA-A2.1²⁵ when peptide 1049 (ALWGFFPVL) is presented.²⁶ Reactivity towards p1049/A2 does not require binding of the TCR co-receptor CD8,²⁷ which allows for the study of TCR-pMHC interactions without the additional complexity of the third protein. We have previously described the crystal structure of the AHIII TCR complexed with p1049/A2.²⁸ From the AHIII-p1049/A2 co-crystal structure, we identified a number of A2 surface residues that may be responsible for binding the AHIII TCR. These residues were mutated in A2 and the changes in T cell cytolytic activity were examined as a function of the mutation. Three mutants were then selected for kinetic, thermodynamic, and structural studies. Most importantly, the K66A mutation causes substantial changes to cytotoxicity and the affinity. This change in affinity appears to be due to a large reduction in hydrogen bonding that is a result of a large conformational change in the CDR3 loop. This loss of hydrogen bonding is reflected in the almost complete loss of enthalpy in the binding reaction.

Results

AHIII T cell reactivity

On the basis of the co-crystal structure of AHIII bound to p1049/A2,²⁸ 13 HLA-A2 mutations were selected to probe the interface. The ability of AHIII T cells to lyse target cells expressing this panel of A2 variants was assessed by loading the target cells with radioactive chromium (⁵¹Cr), incubating the T cells with the target cells for four hours and then measuring the radioactivity released to the medium. Measured lysis was normalized to AHIII lysis of wild-type A2-expressing cells in each experiment. A spectrum of responses to the mutations was seen (Figure 1). Some of the mutants showed little effect on reactivity (E166A and T163A). At the other end of the spectrum, the K66A mutation abolished the response almost completely. In addition to the K66 “hot spot” in A2,^{21–24} it has been suggested that positions 65, 69, and 155 could be critical to MHC-restriction due to the high frequency with which they are seen contacting TCRs in TCR-pMHC structures.^{3,29,30} Consistent with those data, mutations at positions 65, 69, and 155 all had deleterious effects on AHIII cytotoxicity.

Three A2 variants that represent the range of T cell reactivity were chosen for further study: T163A (high), W167A (medium), and K66A (low). Mutant proteins were expressed recombinantly as inclusion bodies in *Escherichia coli* and refolded *in vitro* with peptide p1049. Binding to the recombinant AHIII TCR was measured using SPR. Binding curves for these three complexes in addition to wild-type A2 are shown in Figure 2. The mutations in the MHC cause significant changes to the affinity for AHIII

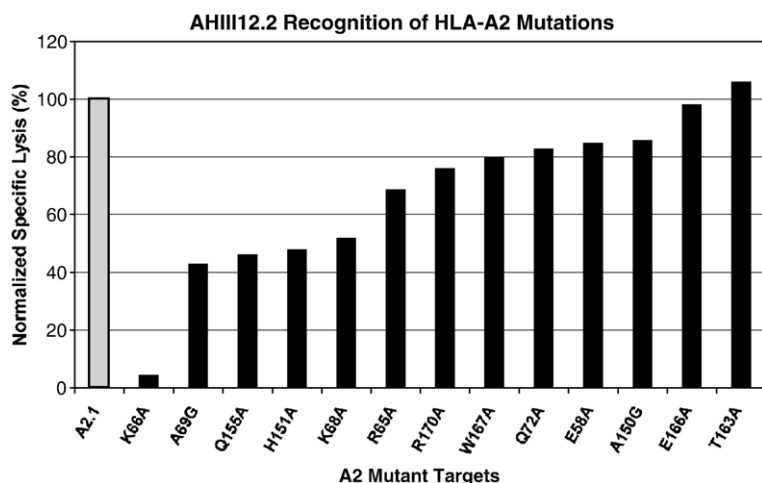


Figure 1. CTL killing as a function of mutations in the p1049/A2 Complex. Cytotoxic lysis assays (^{51}Cr release assays) were performed with AHLII T cells against cells expressing mutant A2. Data were normalized such that lytic activity against native HLA-A2 is 100%.

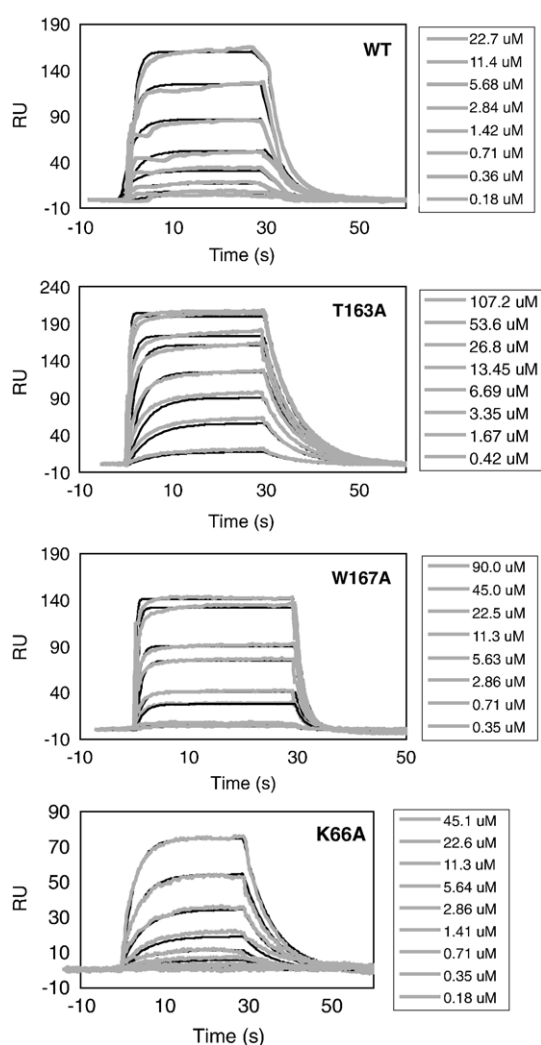


Figure 2. AHLII TCR binding to p1049/A2 variants as measured by SPR. Kinetic data between AHLII TCR and wild-type p1049/A2 as well as p1049/A2 mutants at various concentrations of pMHC were obtained using SPR and globally fit to a reversible bimolecular reaction using Clamp.⁵⁰ Model binding curves are drawn in black. Curve fits are drawn in grey.

TCR (Table 1) with K_d values ranging from 4.7 μM (p1049/A2(T163A)) to 31.8 μM (p1049/A2(K66A)). The kinetics was also dramatically affected. The dissociation rates (k_{off}) were both faster and slower than wild-type p1049/A2 (0.27 s^{-1}). Interestingly, even though the affinity of AHLII for p1049/A2 (K66A) is significantly lower than for wild-type A2, the dissociation rate is significantly slower (Figure 2 and Table 1). Association rates (k_{on}) were generally less affected by the substitutions, except for p1049/A2(K66A) ($4.7 \times 10^3 \text{ M}^{-1}\text{s}^{-1}$), which has a much slower on-rate compared to that of wild-type A2 ($3.1 \times 10^4 \text{ M}^{-1}\text{s}^{-1}$).

Structural analysis of A2 variants

The physical manifestation of the differences found in T cell recognition and binding was examined using X-ray crystallography. The three mutants described above (A2(K66A) A2(T163A) and A2(W167A)) were co-crystallized with AHLII TCR. The locations of the mutations in the interface between the AHLII TCR and p1049/A2 are shown in Figure 3. On the basis of previous work, it seemed unlikely that these relatively small alterations would cause large changes in the overall structures of the TCR or pMHC, or the docking orientation of the TCR.⁵ Therefore, we hypothesized that the substitutions resulted in local alterations in the

Table 1. Equilibrium and kinetic binding parameters for AHLII TCR binding p1049/A2 mutants

pMHC complex	K_d equilibrium (μM)	K_d kinetic (μM)	k_{on} ($\text{M}^{-1}\text{s}^{-1}$)	k_{off} (s^{-1})
p1049/A2	9.3	8.7	3.1×10^4	0.27
p1049/A2(T163A)	4.7	4.6	3.3×10^4	0.16
p1049/A2(W167A)	15.4	14.8	4.1×10^4	0.63
p1049/A2(K66A)	31.8	34.0	0.47×10^4	0.15

Parameters were obtained by fitting data with Scrubber 2.0 and CLAMP.⁵⁰ Kinetic dissociation constants (K_d) were obtained from kinetic data using the determined k_{on} and k_{off} values. Equilibrium dissociation constants were obtained separately by fitting maximum binding responses for various concentrations of pMHC using Scrubber (BioLogic Software, Campbell, Australia).

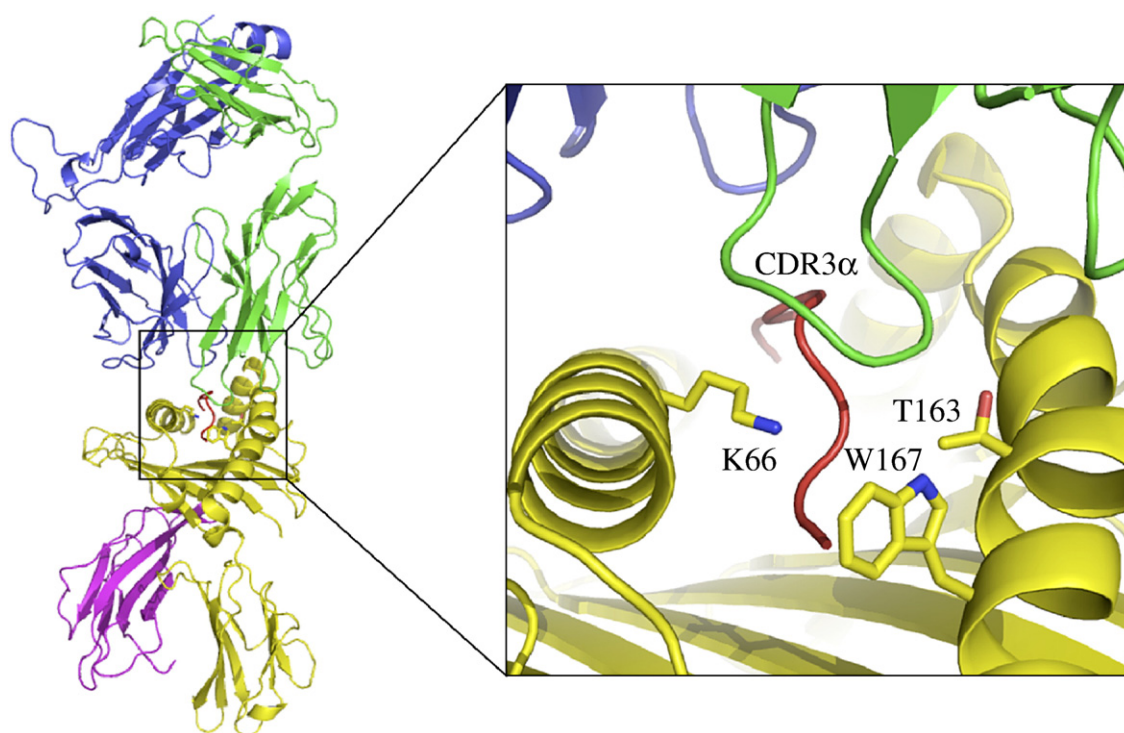


Figure 3. Structure of AHIII TCR bound to p1049/A2. The AHIII TCR α (green) and β (blue) chains, interact with the p1049/A2 surface *via* CDR loops. pMHC, consisting of a heavy chain, A2, (yellow) and β_2m (magenta), present the peptide, p1049 (red). (Inset) The surface of the p1049/A2 is contacted by the CDR loops of the AHIII TCR. Residues that have been mutated to alanine for structural experiments (T163, W167, K66) are shown. The Figure was generated using PDB coordinates 1LP9 and PyMol [<http://pymol.sourceforge.net/>].

MHC or peptide, changing hydrogen bonds or van der Waals contacts present in our previously determined AHIII-p1049/A2 structure.²⁸ Crystallographic data were collected from three single co-crystals comprised of AHIII TCR complexed with p1049/A2(T163A), p1049/A2(W167A), or p1049/A2(K66A), to a resolution of 2.4 Å, 2.5 Å, and 2.88 Å, respectively. All the crystals were nearly isomorphous with AHIII-p1049/A2.²⁸ Data collection and refinement statistics can be found in Table 2.

As might be expected because of the similar level of T cell activity, no gross structural change was observed in the structure of p1049/A2(T163A) bound to AHIII TCR (Figure 4(a)). For all three structures, superimposition was performed using the “align” feature in PyMol†, restraining the alignment to the α -carbon atoms of the TCR-pMHC interface (TCR V α , V β ; and MHC α 1, α 2 and peptide). The AHIII-p1049/A2(T163A) complex superimposed onto AHIII-p1049/A2 with an RMSD of 0.20 Å². Difference electron density ($F_o - F_c$) maps show a large negative electron density peak in the position of the mutated residue, which demonstrates the quality of the data and confirms the location of the mutation (Figure 4(a)). One change in the TCR was observed. The side-chain of serine 99 in the TCR CDR3 α has rotated into the cavity where the MHC threonine side-chain is found in the wild-type structure.

Interestingly, the electron density maps show the location of the serine without ambiguity, but there is no contact visible for the serine side-chain. This side-chain orientation is not the most preferred rotamer;³¹ the preferred conformation is found in the wild-type structure. Therefore, it may be that this position reduces undesired energetic contributions to the binding, such as the fixation of solvent or the production of a cavity in the interface.

In addition to its importance to this study concerning T cell reactivity, the A2(W167A) complex was interesting also because W167 forms a boundary of the peptide-binding cleft (Figure 3) and helps form the conserved pocket that binds the amino terminus of the peptide.³² This tryptophan is highly conserved in HLA-A2 subtypes (96%), and across all human class I MHC molecules (88.5%).³³ Mutating tryptophan to alanine results in the loss of a hydrogen bond between the Trp indole nitrogen atom to the Tyr28 hydroxyl group on the TCR CDR2 (Figure 4(b)). Aside from the loss of the W167-Y28 hydrogen bond, the structure of AHIII bound to p1049/A2(W167A) shows no significant change in the peptide amino terminus, the CDR2 α or CDR3 α of the AHIII TCR, or the MHC itself. The mutant complex alpha carbon atoms have an RMSD of 0.27 Å² when superimposed onto the wild-type atoms. The difference electron density ($F_o - F_c$) map once again shows a large negative peak in the position of the mutated residue demonstrating the quality of the data and confirming the loss of the Trp

† <http://pymol.sourceforge.net/>

Table 2. Data statistics

	AHIII-p1049/ A2(T163A)	AHIII-p1049/ A2(W167A)	AHIII-p1049/ A2(K66A)
A. Data collection			
Space group	$P2_1$	$P2_1$	$P2_1$
Cell parameters			
a (Å)	93.49	94.28	93.42
b (Å)	84.18	84.35	83.89
c (Å)	121.77	122.47	122.27
β (deg.)	92.05	92.53	92.21
Molecules/ asymmetric unit	2	2	2
Resolution (Å)	50.0–2.10	50.0–2.5	50.0–2.88
$R_{\text{merge}}^{a,b}$ (%)	5.9 (46.7)	6.6 (31.8)	7.8 (42.1)
$\langle I/\sigma \rangle^c$	11.4 (1.6)	18.0 (1.8)	11.2 (1.3)
Unique reflections	76,682	61,781	40,707
Average redundancy	2.7 (1.7)	4 (2.5)	3.4 (2.3)
Completeness (%)	70.0 (24.7)	92.8 (67.8)	95.7 (69.0)
Solvent content (%, v/v)	41.5	40.7	44.1
B. Refinement			
Resolution range (Å)	30.0–2.4	30.0–2.5	30.0–2.88
No. reflections	59,694	58,660	38,683
R_{fac}^d	24.0	25.3	26.8
R_{free}^d	28.9	29.9	29.3
No. non-H atoms	13,160	12,995	12,956
No. water molecules modeled	267	52	0
$\langle R_s \text{ fit} \rangle^e$	93%	93%	90%
Coordinate error ^{f,45,46}	0.25	0.32	0.46
RMS deviations from ideality			
Bond lengths (Å)	0.006	0.006	0.005
Bond angles (deg.)	1.040°	1.192°	0.750°
$\langle \text{Temperature factor} \rangle$			
Overall	37.6	49.7	47.2
TCR	37.8	49.6	47.5
MHC	37.6	50.1	47.1
Peptide	34.7	48.6	37.5
Ramachandran plot			
Most favored (%)	91.4	90.7	90.4
Additionally allowed (%)	8.5	9.2	9.4
Generously allowed (%)	0	0	0
Disallowed (%)	0.1	0.1	0.1
PDB entry	2UWE	2JCC	2J8U

^a $R_{\text{merge}} = \sum_{hkl} \sum_i |I_i - \langle I \rangle| / \sum_{hkl} \sum_i I_i$, where I_i is the observed intensity and $\langle I \rangle$ is the average intensity of multiple observations of symmetry-related reflections.

^b Numbers in parentheses refer to the highest resolution shell.

^c $I/\sigma I$ for the highest resolution shells: 2.49–2.37 Å, 2.59–2.50 Å, 3.0–2.9 Å (T163A, W167A, and K66A, respectively).

^d $R = \sum_{hkl} ||F_{\text{obs}}| - k|F_{\text{calc}}|| / \sum_{hkl} |F_{\text{obs}}|$, where R_{free} is calculated for a randomly chosen 5% of reflections, and R_{work} is calculated for the remaining 95% of reflections used for structure refinement.

^e $\langle R_s \text{ fit} \rangle$ is the average real space fit of all atoms on a $2F_{\text{obs}} - F_{\text{calc}}$ electron density map.

^f Error is the mean coordinate error estimate based on maximum likelihood measurements.

side-chain. Two side-chains in A2 near the site of mutation do change conformation, but these differences do not alter binding to the TCR. The amino terminus of the peptide is still coordinated by hydrogen bonds to three tyrosine hydroxyl groups Tyr7, Tyr 159, and Tyr171 of the MHC, as in wild-type p1049/A2. The AHIII-p1049/A2(W167A) structure shows weak positive difference density in the

location where the nitrogen atom of the indole ring of wild-type Trp167 would be (data not shown). This suggests that there may be a weakly associated water molecule replacing the amine, which could hydrogen bond to the hydroxyl group on Tyr28 of CDR2 α .

The structure of AHIII bound to p1049/A2(K66A) is critical to this study because of the significantly different binding constants of p1049/A2(K66A) (Table 1). Additionally, K66 on the $\alpha 1$ α helix of HLA-A2 has been identified as a “hot spot” for TCR recognition of HLA-A2 in a number of studies.^{21–24} Structures of A6-Tax/A2,^{10,34} and AHIII-p1049/A2²⁸ also show that K66 is rare, in that it makes critical contacts with both the TCR and the peptide. K66A mutants have increased peptide dissociation rates; yet this is not likely to be responsible for the decrease in T cell function because T cell clones have been identified that do not have altered recognition to the K66A mutation.^{21,22} Furthermore, the K66A mutation does not alter the MHC structure or the conformation of the Tax peptide in Tax/A2(K66A).²⁴ So, if increased peptide dissociation from A2(K66A) mutants does not influence T cell activation, and the pMHC molecular surface is not altered by the mutation, the next logical hypothesis would be that the K66A variation results in a change in the TCR that negatively affects T cell function.

The co-crystal structure of AHIII-p1049/A2 (K66A) determined to 2.88 Å resolution shows an altered conformation of the CDR3 α of the AHIII TCR (Figure 4(c)). The AHIII-p1049/A2(K66A) structure superimposes onto AHIII bound to wild-type A2 with an RMSD of 0.37 Å². The $2F_o - F_c$ electron density map shows the new conformation of the loop (Figure 4(d)) and this location is confirmed by omit maps. The conformational change in CDR3 α is that the loop appears to fill the void left by the removal of the Lys66 side-chain. The C α atoms of the loop move, on average, 2.0 Å with Ala97 moving over 4.0 Å (Table 3). This altered conformation of the loop likely disrupts the hydrogen bonding contacts found in the native structure between the CDR3 α and wild-type p1049/A2 (Figure 4(e)).²⁸ In a manner similar to the Tax/A2(K66A) structure,²⁴ the K66A mutation does not change MHC or peptide conformation in this AHIII-p1049/A2(K66A) structure. The CDR3 loop change negatively affects the surface complementarity (SC). The SC value for the wild-type AHIII-p1049/A2 structure is 0.71 and drops to 0.55 for AHIII-p1049/A2(K66A).

The Tax/A2(K66A) structure showed a water molecule replacing the Lys66 side-chain, mediating hydrogen bonds between Glu63 of A2 and the Tax peptide.²⁴ There is no electron density that would suggest a water molecule replaces the Lys66 side-chain in our AHIII-p1049/A2(K66A) structure. It appears that the new conformation of the CDR3 α loop pushes further into the peptide-binding cleft along the MHC $\alpha 1$ α helix, where the Lys66 side-chain would have been, displacing any water that might have filled the void before TCR binding. The number of reflections associated with the

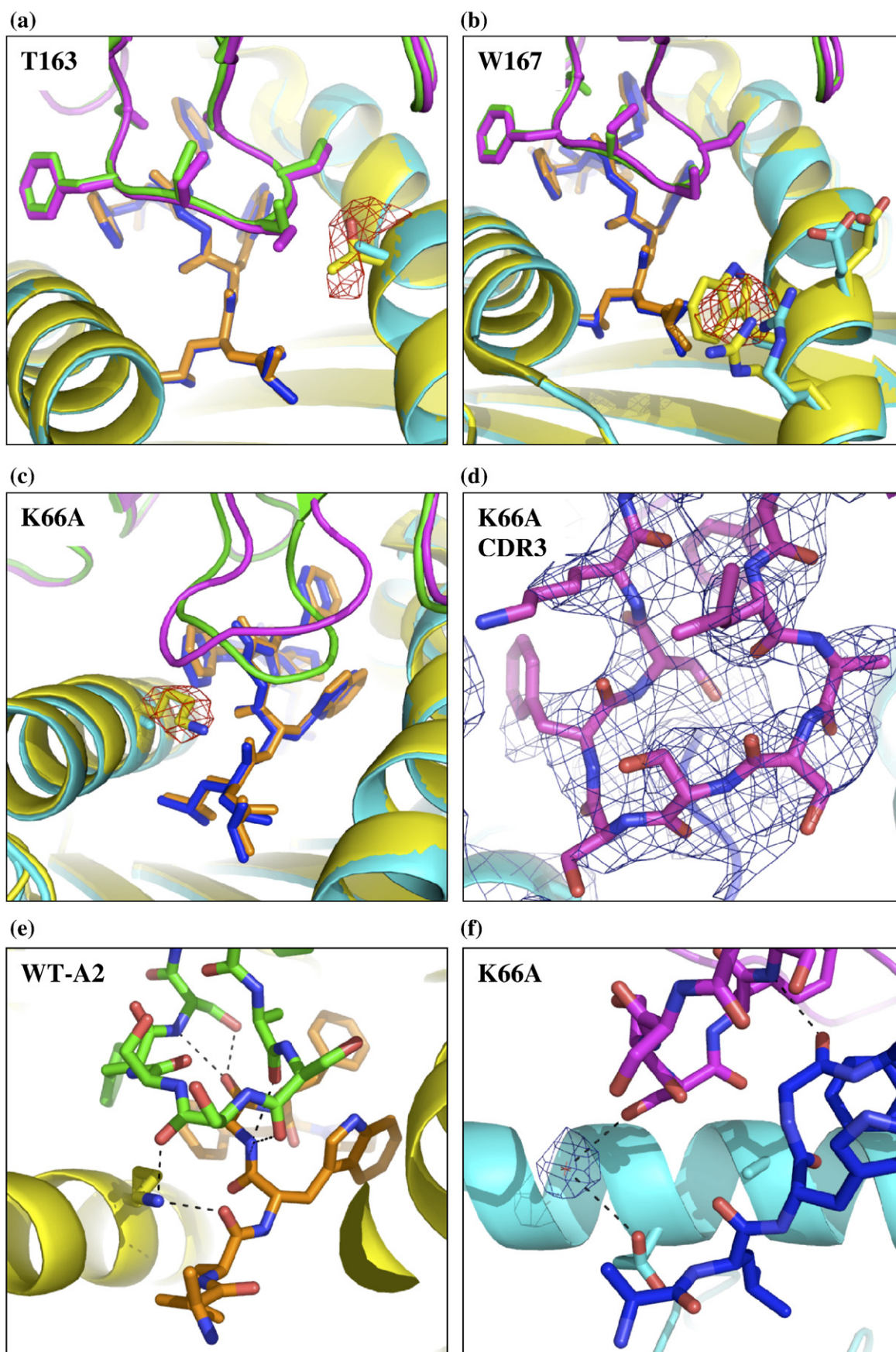


Figure 4 (legend on next page)

Table 3. CDR3 α movement

Residue	Distance (Å)
Leu96	1.0
Ala97	4.2
Ser98	2.6
Ser99	3.0
Ser100	2.6
Phe101	0.3
Ser102	1.7
Lys103	0.7
Mean	2.0

Distances are limited to two significant figures due to the low resolution of AHIII-p1049/A2(K66A).

2.88 Å resolution data cannot support the modeling of water molecules in the structure of AHIII-p1049/A2(K66A). However, there is a small peak in the $2F_o - F_c$ electron density map that suggests that there may be a weakly associated water molecule that would hydrogen bond with Glu63 of A2 and Ser100 on CDR3 α of AHIII (Figure 4(f)). The only other plausible hydrogen bond between the AHIII CDR3 α to p1049/A2(K66A) is from the Ser102 nitrogen atom to the Gly4 oxygen atom of the peptide (2.88 Å) (Figure 4(f)). In summary, there is a large alteration in the AHIII CDR3 α loop when bound to p1049/A2 (K66A) as compared to the wild-type complex, and this alteration appears to dramatically change the number of hydrogen bonds in the complex.

Calorimetric measurement of AHIII TCR and HLA-A2 binding

The altered hydrogen bonding pattern proposed here on the basis of the crystal structure of AHIII-p1049/A2(K66A) suggests that there should be a large change in the enthalpy of binding. To examine this directly, the heat of binding was measured using ITC. Our data show that the wild-type complex binding has a relatively small enthalpic component (−3.9 kcal/mol) and that the binding is more entropically driven (Table 4 and Figure 5(a)). As predicted, this small enthalpic contribution to binding is almost completely eliminated by mutation of K66 to alanine. This change is manifest clearly during the experiments because the K66A

mutation changes the reaction from exothermic to endothermic (Figure 5(b)). The enthalpy of binding (ΔH) goes from −3.9 kcal/mol for AHIII-p1049/A2 to almost zero (−0.6 kcal/mol) for AHIII-p1049/A2 (K66A). The free energy of binding (ΔG) measured for the two complexes is in agreement with those determined for other TCR-pMHC (Table 4). The thermodynamic changes for AHIII-p1049/A2(K66A) correspond to a $\Delta\Delta G$ of only 1.4 kcal/mol, which highlights the tight range between activating and non-activating signals for TCR.

Discussion

The initial goal of this study was to determine how structural alterations in the TCR are responsible for the spectrum of T cell cytotoxicity by AHIII T cells. Mutations in HLA-A2 were made and changes in cytotoxicity examined as a function of the mutation. Recombinant protein for three A2 variants was produced, and binding constants were determined by SPR. Surprisingly, A2(K66A) showed very different kinetic constants as compared to the wild-type complex. Structural studies showed that most hydrogen bonds involving the CDR3 α loop in the complex were lost upon mutation. ITC confirmed a greatly decreased enthalpy of binding associated with the conformational change of the loop.

On the basis of the AHIII-p1049/A2 co-crystal structure,²⁸ A2 residues that were predicted to be involved in binding the AHIII TCR were mutated. The AHIII T cells reacted with a full spectrum of outcomes from very low cytotoxicity to slightly improved cytotoxicity as a result of changing residues in the interface between the proteins. Residues at positions 66^{21–24} and 65, 69 and 155^{3,29,30} have all been identified as critical contacts in a number of TCR-pMHC systems. Mutations at all four of these positions in A2 resulted in a reduction of AHIII T cell cytotoxicity of 30% to almost 100%. Clearly, these residues are critical for AHIII TCR binding. As an important control, it has been shown that peptide binding does not change significantly for the mutations studied except K66A (it has a faster peptide off-rate).²² However, this faster peptide off-rate cannot account for the

Figure 4. Mutation of Lys66 to alanine results in a large change in the CDR3 α loop. (a) The complex of AHIII TCR bound to p1049/A2(T163A) superimposed on the wild-type structure of AHIII-A2. Mutant A2 (cyan) and peptide (blue) show little difference from wild-type A2 (yellow) or peptide (orange). The conformations of TCR CDR2 and CDR3 loops and side-chains are not different between the mutant (magenta) and wild-type (green) structures (the coloring scheme is the same throughout the Figure). (b) The complex of AHIII TCR bound to p1049/A2(W167A) also shows no change in TCR structure and only minor alterations in local MHC side-chains. (c) Superimposition with of AHIII TCR bound to p1049/A2(K66A) onto wild-type shows a major rearrangement of the AHIII CDR3 α loop, while the structure of pMHC is unchanged. (a)–(c) Mutations at T163A, W167A, and K66A are confirmed by difference electron density ($F_o - F_c$) contoured at -3σ surrounding the side-chains. (d) The $2F_o - F_c$ density map (blue), contoured at 1 σ , confirms placement of the final modeled CDR3 α loop at 2.88 Å. (e) Five hydrogen bond interactions occur between AHIII TCR CDR3 α and wild-type p1049/A2. As shown above, some or all of these bonds may be broken due to loop movement. (f) The $2F_o - F_c$ electron density suggests the presence of a water molecule in the AHIII-p1049/A2(K66A) structure, which would allow for a water-mediated hydrogen bond between Glu63 of A2 and Ser100 on CDR3 α of AHIII (water is shown for illustration, but is not included in PDB). The only other possible hydrogen bond to CDR3 α is from the Ser102 nitrogen atom to the Gly4 oxygen atom of the peptide. The Figure was generated using PyMol [<http://pymol.sourceforge.net/>].

Table 4. Thermodynamic parameters of TCR-pMHC binding as measured by ITC

Complex	ΔH (kcal/mol)	$T\Delta S$ (kcal/mol)	ΔG (kcal/mol)	K_d (μ M)	Reference
AHIII-p1049/A2	-3.9 ^a	4.4	-8.3	1 \pm 5	
AHIII-p1049/A2(K66A)	-0.6 ^b	6.3	-6.9	7 \pm 20	
A6-Tax/A2	5.7	13.6	-7.9	2.2	18
JM22-flu/A2	-19.7	-12.6 ^c	-7.1 ^c	6.6 ^c	15
2C-dEV8/K ^b	-22.7	-16.2	-6.3	84	17
2C-QL9/L ^d	-4.19	3.4	-7.6	2	19
LC13-FLR/B8	-3.6	3.4	-7.0	8.1 \pm 2.7	17
2B4-MCC/IE ^k	-14.8	-8.2	-6.7	12.6 \pm 7	14
2B4-K5/IE ^k	-13.5	-6.4	-7.2	6.2 \pm 0.2	14

^a Error <5%.^b Error <20%.^c van't Hoff calculation.

changes in activity because T cells can be found that are not affected by the K66A mutation.^{21,22} This implies that significant peptide bound to MHC remains on the cell surface even with the K66A mutation. In addition, the levels of expression of the various mutants studied here were confirmed to be similar by flow cytometry (data not shown). Therefore, any observed changes in reactivity, binding, or structure should be due to changes in how the complexes interact. A more thorough study of how those mutations resulted in a change of function was then initiated.

A sub-set of the MHC mutants that represent dramatically reduced to full reactivity (K66A, W167A, and T163A, respectively) were chosen to study the physical manifestation of the differences. TCR-pMHC binding studies were performed using SPR. While all mutants showed some degree of change from wild-type A2, the K66A mutation resulted in remarkably slower on and off-rates than the wild-type complex. The three mutant complexes were then co-crystallized with AHIII TCR. The structures were determined and compared to the wild-type co-crystal structure. Similar to the results seen for the altered peptide ligands for the Tax/A2 specific TCR,⁵ there was no gross differences in any of the structures examined. Significantly, there was no change in domain packing of the TCR that would suggest a mode to transmit information through the domains to the interior of the cell to confer different activities, as previously suggested.¹⁴ There is always the possibility that the domain movements are dynamic and/or weakly manifested, and are overcome here by crystal packing forces that would make it impossible to view using protein crystallography. Similarly, it has been suggested that upon TCR-pMHC interaction, a conformational change in the AB loop of the TCR C α domain is required for signaling into the cell.⁸ Although the position of the AB loop for the non-liganded AHIII TCR is unknown, the loop in the AHIII TCR bound to all p1049/A2, even p1049/A2(K66A), is identical, and is the same conformation as that seen in the liganded LC13 TCR.⁸ Importantly, the AB loop in the AHIII structures are not involved in any crystal contact. These data imply that the AB loop has no impact on the level of cytotoxicity seen in the AHIII system.

There is no definitive structural explanation for the "improved" AHIII T cell reactivity for the A2 (T163A) mutant. With threonine being conserved in 98% of all known HLA-A2 subtypes,³³ we had expected a greater impact mutating it to alanine. If anything, the rotation of the TCR CDR3 α Ser99 into the cavity formed by the removal of the MHC threonine side-chain would be expected to contribute negatively to the binding due to the less favorable rotamer that is chosen. There is no hydrogen bonding partner near the new position of the serine hydroxyl group. There is no significant increase in the complementarity in the fit between the complexes. The complementarity of fit of AHIII to p1049/A2(T163A) is 0.72 *versus* 0.71 for the wild-type structure. We conclude that the most likely explanation for the slightly increased binding affinity is that there is a set of very subtle changes that increase the complementarity of fit.

The A2(W167A) mutation results in a 20% loss in lysis by the AHIII T cells. There is no significant structural change other than the loss of the W167-Y28 hydrogen bond. Loss of the W167 indole group also affects surface complementarity between AHIII-p1049/A2(W167A) (SC=0.68) compared to AHIII-p1049/A2 (SC=0.71). Therefore, the dramatic loss of affinity to the AHIII TCR is likely a result of the lost hydrogen bond and the concomitant loss of complementarity (i.e. van der Waals contacts). The fact that the absence of the indole group from the end of the peptide-binding cleft in the AHIII-p1049/A2(W167A) structure did not significantly alter the conformation of the bound peptide is surprising. Tryptophan is present at position 167 in 96% of all known HLA-A2 subtypes and 88.5% conserved in all human class I MHC molecules.³³ It begs the question, why is this amino acid so highly conserved? Unfortunately, the data provided in the AHIII-p1049/A2(W167A) structure are unable to address this.

Of all the mutants tested, the K66A mutation caused the largest decrease in AHIII cytotoxicity. The slow on-rate seen for AHIII-p1049/A2(K66A) and significant energy barriers measured for other TCR-pMHC^{35,36} imply that there are structural changes associated with binding and, in fact, a large change was seen in the CDR3 α loop of the AHIII TCR. This

suggests that binding requires a conformational change in the TCR, but when exactly does this occur? Does the AHIII TCR make initial contact with p1049/A2(K66A) and then the CDR3 α loop moves

(induced fit) or does p1049/A2(K66A) associate with a minority member of the population of the AHIII TCRs in solution (pre-existing equilibrium). The induced-fit or two-step model has been a popular means of describing TCR-pMHC interaction.³⁷ However, the validity of the two-step model has been questioned by both thermodynamic³⁵ and structural^{8,9,12} data. We propose that a pre-existing equilibrium model better describes TCR-pMHC association. The idea that CDR loops exist in alternative pre-existing conformations in solution has been shown in antibody crystal structures.³⁸ Knowing the structural similarities between antibodies and TCR, it is easy to imagine this binding mechanism to exist for TCR and pMHC. The total number of possible conformations that the CDR loops can adopt is finite and limited by the conserved framework regions of the TCR and/or antibody structure.^{39–42} The residues that constitute the loop will maintain ϕ and ψ angles that allow for the lowest potential energy. Loops in higher potential energy conformations would be found less often in the population (minority member). Therefore, the pMHC surface that allows the TCR to have the greatest number of its CDR loops in conformations with the lowest energy would provide the most stable interaction, a higher affinity, and subsequent greater activation of the T cell. The structural and thermodynamic data presented here for AHIII TCR-p1049/A2(K66A) demonstrate this relationship between energetics and activation. When the CDR3 α loop is required to take a conformation with higher energy, the interactions between TCR and pMHC suffer, and T cell activation is adversely affected. As the structure of AHIII TCR alone is not available, we cannot be sure where the CDR3 α loop lies when it is free in solution. However, the on-rate of AHIII-p1049/A2(K66A) being an order of magnitude slower than wild-type AHIII-p1049/A2 binding, suggests the loop to undergo greater change in order to bind p1049/A2(K66A) than wild-type p1049/A2. We propose the TCR conformations seen in our AHIII-p1049/A2(K66A) complex are minor in the population, so the longer k_{on} is a reflection of the un-

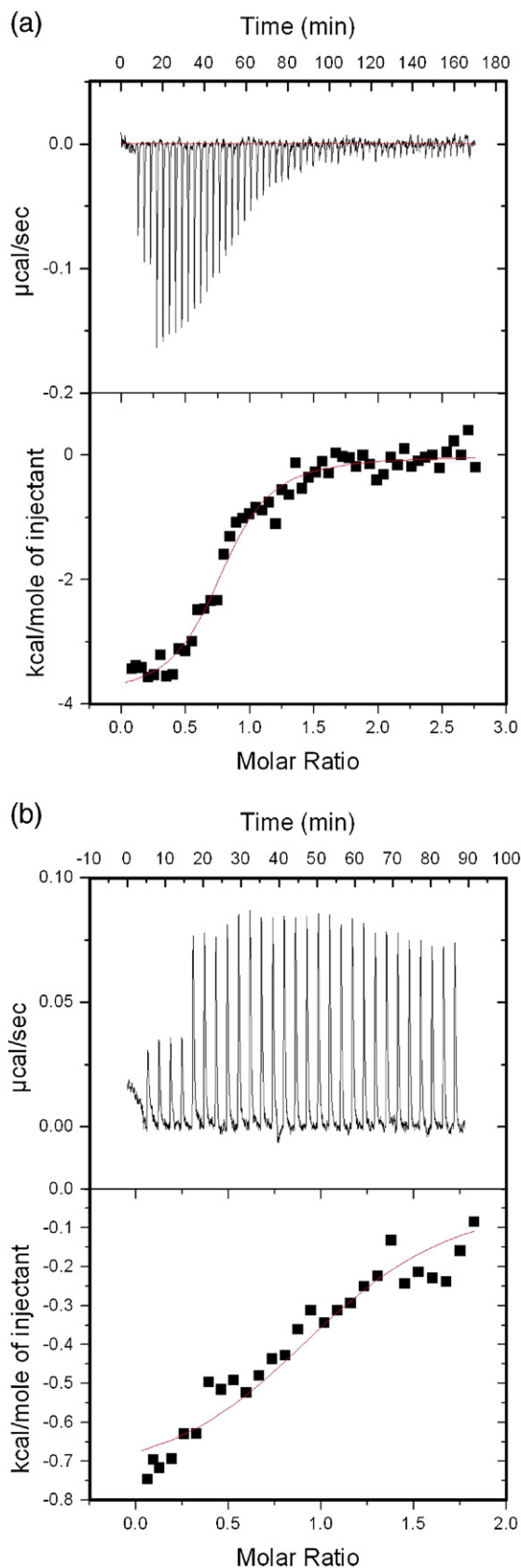


Figure 5. K66A mutation in p1049/A2 decreases the enthalpy of binding dramatically. The binding enthalpy of AHIII TCR was measured directly with ITC for both wild-type p1049/A2, and p1049/A2(K66A). (a) A power versus molar ratio plot for titration of 234 μ M p1049/A2 into 19 μ M of AHIII TCR (upper panel) and a plot of integrated heat versus molar ratio after baseline correction (lower panel). The baseline was generated by averaging heat measured for the last ten injections. (b) A plot of power versus molar ratio for titration of 394 μ M p1049/A2(K66A) into 40 μ M of AHIII TCR (upper panel) and integrated heat versus molar ratio after baseline correction (lower panel). The baseline derived from titrating p1049/A2(K66A) into buffer alone. All experiments were done at 25 $^{\circ}$ C. The fitted curves are from the model for single-site binding provided in Microcal Origin Software. The thermodynamic parameters determined are given in Table 4.

favorable equilibrium of the pMHC binding that minority member.

The AHIII-p1049/A2(K66A) structure also suggested most of the hydrogen bonds found between AHIII CDR3 α and wild-type p1049/A2 are not present in the mutant structure. The conformational change in CDR3 α potentially leaves only the Ser102 to Gly4 hydrogen bond. This suggested that the enthalpy of binding is greatly diminished. The ITC data complement the structural data, as they show there is a significant loss in binding enthalpy. Due to the small amount of heat absorbed upon AHIII-p1049/A2(K66A) binding, the titration curve generated does not allow for confident analysis of the entropy in the system. However, the endothermic binding combined with the loss of enthalpy suggests that the binding of AHIII TCR to p1049/A2(K66A) is nearly entirely entropically driven. For TCR-pMHC complexes where heats of binding have been measured directly (and inferred from van't Hoff calculations), the enthalpic and entropic contributions are different for each TCR-pMHC system without any unifying thermodynamic properties. Originally it was thought that TCR-pMHC interactions were governed by enthalpically favorable and entropically unfavorable thermodynamics features;^{13–15} however, AHIII-p1049/A2 joins LC13-FLR/B8,¹⁷ A6-Tax/A2,¹⁸ and 2C-QL9/L^{d19} as TCR-pMHC systems that rely on entropically favorable binding.

One of the difficulties associated with studying diverse receptor systems such as TCR recognition of pMHC is that it is difficult to extract general rules about the system. However, in the context of what has been done with other TCR-pMHC, there are some general features that we can present from these data. Previous structural studies have highlighted TCR recognition of altered peptide ligands,^{5,12} different peptides presented by the same MHC,^{4,6,9,43} or the effects of mutation in the TCR to binding,⁴⁴ but not the structural effects of MHC mutation on TCR-pMHC binding. The effects of mutations in the MHC through biological readout, co-crystal structures, and thermodynamics suggest a correlation between T cell response and affinity. As many as 32 hydrogen bonds determine specificity in BM3.3-pBM1/K^b,⁴³ but only 21 in AHIII-p1049/A2²⁸ and approximately 15 in the AHIII-p1049/A2(K66A) complex. The recently determined structure of 2C-QL9/L^{d19} reveals an interface with less than ten hydrogen bonds and entropically favorable binding. What does this say about specificity? If there are no hydrogen bonds determining specificity, the only way the TCR can be sure to recognize only the foreign complex must be complementarity of fit. Not surprisingly perhaps, AHIII-p1049/A2²⁸ and 2C-QL9/L^{d19} have the greatest complementarity of fit of all TCR-pMHC structures determined to date. In addition to other published results, our data suggest that the thermodynamics for each TCR-pMHC interaction is unique. The large range of thermodynamic constants reveals that there are many ways to induce T cell activation. This all suggests that the

pathways to activation are not important, just the end point.

Most importantly, the AHIII-p1049/A2(K66A) structure provides evidence that a variation in the MHC and not the peptide can directly affect a CDR3 loop. The idea of CDR1 and CDR2 recognition of MHC followed by CDR3 binding to peptide works for a select few TCR, but not for most. In the case of K66, Lys is not conserved across all MHC (93% of HLA-A2 subtypes, but only 42.5% conserved in HLA-A overall, and only 1.5% of HLA-B molecules³³). Therefore, the presence of this charge is not required, but can be thought of as another piece of the antigen surface. TCR recognition of the pMHC surface cannot be divorced into separate binding events of peptide and MHC.

Materials and Methods

Cell lines

The HLA-A2 mutants transfected into Hmy2.C1R cells have been described.²³ All cell lines showed cell surface expression of HLA-A2 at levels similar to that of wild-type HLA-A2 as detected by the HLA-A2-specific Ab BB7.2.⁴⁷

Protein production and purification

Soluble AHIII12.2 TCR was produced as described.²⁸ Briefly, the ectodomains of AHIII TCR α and β chains were expressed as inclusion bodies in *E. coli*. Purified inclusion bodies, previously dissolved in 8M urea, were injected rapidly into a folding buffer optimized for the AHIII TCR at a final concentration of 50 μ g/ml. After incubation for 36 h at 10 °C and extensive dialysis, the native TCR was purified and concentrated by DE52 anion-exchange chromatography (Whatman, Florham Park, NJ) followed by gel-filtration chromatography (Phenomenex, Torrance, CA) on HPLC. The purified AHIII TCR was concentrated to 10 mg/ml and stored at –80 °C. Soluble AHIII TCR was tested for proper folding and activity through an ELISA using HLA-A2 tetramer. Typical yield for each 1 l of refold is about 3–5 mg of active TCR.

Similarly, soluble HLA-A2 variants were produced as inclusion bodies in *E. coli* and refolded *in vitro*.⁴⁸ Peptide p1049 (ALWGFFPVL), presented by A2, was synthesized by the UNC Peptide Synthesis Facility (Chapel Hill, NC). Briefly, peptide, β_2 m, and heavy chain were injected in that order into a folding buffer optimized for refolding class I MHC at a concentration of 50 μ g/ml. After incubation for 24–36 h at 10 °C the folded pMHC was concentrated in an Amicon ultrafiltration cell (Millipore, Billerica, MA) and purified using gel-filtration chromatography (Phenomenex) on HPLC. The purified wild-type and A2 variants were concentrated to 10 mg/ml and stored at –80 °C. Typical yield for each 1 l of refold is about 5 mg of pMHC.

Cytotoxicity assay

Cytotoxicity was assayed using a standard 4 h ⁵¹Cr release assay as described.⁴⁹ Briefly, between 5.0 \times 10³ and 5.0 \times 10⁴ AHIII 12.2 T cells were incubated with 5000 peptide-pulsed ⁵¹Cr-labeled A2 mutant-transfected cells.

Since p1049 is a human self-antigen, the transfectants were recognized without the addition of p1049 to the cells. Additional p1049 did not increase cytotoxicity (data not shown).

Surface plasmon resonance experiments

Five-thousand resonance units (RUs) of H57-597 (capturing molecule, anti-TCR C β Ab) were covalently bound to a Biacore CM5 sensor chip (Uppsala, Sweden) using standard amine coupling. Soluble AHIII12.2 TCR (ligand) was then added to the Ab at a final concentration of 50–100 nM to generate 300–400 RU of bound TCR. Soluble class I MHC (analyte) was injected onto the surface at a flow-rate of 100 μ l/min in a 30 s pulse. TCR and MHC were removed from the surface with 0.1 M glycine (pH 2.5), 0.5 M NaCl and the procedure was repeated until at least three curves were obtained for the different concentrations of analyte. Curves obtained at each concentration were subtracted from a reference surface that contained Ab alone without TCR or using recombinant P14 TCR as a negative control. Data were processed using Scrubber (BioLogic Software, Campbell, Australia) and CLAMP.⁵⁰ The suitability of the fit was measured based on χ^2 values and the appearance of residuals. In all cases, χ^2 was <1, residuals were small and random, and the experimental curves visually matched the predicted curves.

Protein crystallization and structure determination

The crystallization conditions for the crystal complexes were similar to those optimized for AHIII TCR with wild-type A2.²⁸ Briefly, crystals were grown by hanging-drop, vapor-diffusion, using AHIII TCR and A2 variants mixed at equal ratios at a concentration of 10 mg/ml. Drops contain 1 μ l of protein solution mixed with 1 μ l of a well solution containing 25 mM Hepes (pH 7.5–8.0), 1 M NaCl, 14–18% (w/v) PEG 8000. Small crystals formed within three days along with precipitate in the drops. Crystal size was improved by macro-seeding under identical conditions. Crystals were transferred to mother liquor containing 25% (v/v) glycerol as cryoprotectant. Crystallographic data were collected at the Southeast Regional Collaborative Access Team (SER-CAT) 22-ID and 22-BM beamlines at the Advanced Photon Source, Argonne National Laboratory (Argonne, IL). Data for AHIII-p1049/A2(T163A) were collected on the 22-BM beamline at 12,398.42 eV for 360° at a distance of 200 mm using 1.0° oscillations. Two datasets for AHIII-p1049/A2(W167A) were collected on the 22-ID beamline at 12,759.89 eV at a distance of 300 mm using 1.0° oscillations: a 180° dataset was collected at an ω angle of 90° and an additional 45° dataset was collected at an ω angle of 45°. These datasets were indexed separately and then scaled together. Data for AHIII-p1049/A2(K66A) were collected on the 22-ID beamline at 12,759.89 eV for 180° at a distance of 300 mm using 1.0° oscillations. Data for all co-crystal complexes were indexed and scaled with HKL2000.⁵¹ The dataset for AHIII-p1049/A2(T163A) was collected originally out to 2.1 Å, but it was highly anisotropic. As a result, the statistics in the highest shells were poor, so the dataset was truncated at 2.4 Å. Molecular replacement solutions were determined using rigid body refinement in Refmac 5.0,⁵² with AHIII-p1049/A2 (1LP9) as the search model.²⁸ Temperature factors were set to 30.0 using Moleman.⁵³ Positional refinement using non-crystallographic symmetry restraints for the first few cycles and

TLS refinement⁵⁴ in Refmac 5.0 was performed iteratively with manual intervention with O.⁵⁵ When the statistics did not improve over two subsequent rounds of refinement and the R_{free} value was below 30%, water molecules were added using Arp within Refmac 5.0 to AHIII-p1049/A2(T163A) and AHIII-p1049/A2(W167A) models. All water molecules were examined to confirm the presence of hydrogen bond donors or acceptors at reasonable geometries. For the AHIII-p1049/A2(K66A) model, an omit map of the CDR3 α loop was generated to verify the conformational change. The refinement statistics for the final models are presented in Table 2. Surface complementarity (SC) values were calculated using Sc⁵⁶ in the CCP4 suite.⁵²

Isothermal titration calorimetry

ITC experiments on AHIII TCR with wild-type p1049/A2 and p1049/A2(K66A) were performed on a Microcal VP-ITC in the UNC Macromolecular Interactions Facility (Chapel Hill, NC). Thermodynamic constants were obtained for AHIII TCR binding wild-type p1049/A2 as well as p1049/A2(K66A) by fitting the calorimetric data using a one-site binding model in Microcal Origin version 5.0 Software (OriginLab Corporation, Northampton, MA). Soluble AHIII TCR was placed in the mixing chamber. p1049/A2 or p1049/A2(K66A) was titrated into the AHIII TCR solution until binding reached saturation. Titration of wild-type p1049/A2 into AHIII TCR was performed in duplicate, once in 10 mM sodium phosphate buffer (pH 7.5), and then in 10 mM Tris-HCl buffer (pH 7.5), to ensure that the determined enthalpy was not affected by ionization enthalpy of the buffer.⁵⁷ Concentrations of AHIII TCR and p1049/A2 were 17 μ M and 217 μ M, respectively, in the phosphate buffer and 19 μ M and 234 μ M, respectively, in the Tris buffer. For wild-type p1049/A2 experiments, a volume of 3 μ l was used for the first four injections, and then 5 μ l for the remaining titrations. The baseline, generated by averaging the heat measured for the last ten injections, was subtracted from all peaks. Titration of p1049/A2(K66A) in AHIII TCR was performed in triplicate in the phosphate buffer. Concentrations of AHIII TCR and p1049/A2(K66A) were 40 μ M and 618 μ M, 65 μ M and 450 μ M, and 43 μ M and 394 μ M, respectively, for the three replicates. For all p1049/A2 (K66A) experiments, a volume of 5 μ l was injected for the first four peaks, increased to 10 μ l for the remainder of the experiment. Because of the relatively small amount of heat released upon AHIII-p1049/A2(K66A) binding, a more accurate baseline was determined by injecting p1049/A2 (K66A) into the phosphate buffer to measure the heat of dilution. This reference dataset was subtracted from the experimental dataset in Origin Software. All concentrations were determined before the proteins were placed in the microcalorimeter using extinction coefficients. ΔH and ΔS were calculated using the Origin software. Gibbs free energy was calculated as $\Delta G = \Delta H - T\Delta S$, where $T = 298$ K.

Acknowledgements

We thank Dr William E. Biddison of the Molecular Immunology Section of the National Institutes of Health, Bethesda, MD for supplying the HLA-A2 variant cells lines for our cytotoxicity assays. Data

were collected at the Southeast Regional Collaborative Access Team (SER-CAT) 22-ID beamline at the Advanced Photon Source, Argonne National Laboratory. Staff at the beamline are acknowledged for assistance in data collection. Use of the Advanced Photon Source was supported by the U. S. Department of Energy, Office of Science, Office of Basic Energy Sciences, under contract no. W-31-109-Eng-38. The director of the UNC Macromolecular Interactions Facility, Dr. Ashutosh Tripathy, Ph.D. is gratefully acknowledged for his assistance with collecting and interpreting ITC data. Members of the Collins and Frelinger labs are acknowledged for helpful discussions. Funding provided by NIH grant CA92368-02.

References

- Schatz, D. G. & Spanopoulou, E. (2005). Biochemistry of V(D)J recombination. *Curr. Top. Microbiol. Immunol.* **290**, 49–85.
- Spicuglia, S., Franchini, D. M. & Ferrier, P. (2006). Regulation of V(D)J recombination. *Curr. Opin. Immunol.* **18**, 158–163.
- Rudolph, M. G., Stanfield, R. L. & Wilson, I. A. (2006). How TCRs bind MHCs, peptides, and coreceptors. *Annu. Rev. Immunol.* **24**, 419–466.
- Degano, M., Garcia, K. C., Apostolopoulos, V., Rudolph, M. G., Teyton, L. & Wilson, I. A. (2000). A functional hot spot for antigen recognition in a superagonist TCR/MHC complex. *Immunity*, **12**, 251–261.
- Ding, Y. H., Baker, B. M., Garboczi, D. N., Biddison, W. E. & Wiley, D. C. (1999). Four A6-TCR/peptide/HLA-A2 structures that generate very different T cell signals are nearly identical. *Immunity*, **11**, 45–56.
- Garcia, K. C., Degano, M., Pease, L. R., Huang, M., Peterson, P. A., Teyton, L. & Wilson, I. A. (1998). Structural basis of plasticity in T cell receptor recognition of a self peptide-MHC antigen. *Science*, **279**, 1166–1172.
- Reiser, J. B., Gregoire, C., Darnault, C., Mosser, T., Guimezanes, A., Schmitt-Verhulst, A. M. *et al.* (2002). A T cell receptor CDR3 β loop undergoes conformational changes of unprecedented magnitude upon binding to a peptide/MHC class I complex. *Immunity*, **16**, 345–354.
- Kjer-Nielsen, L., Clements, C. S., Purcell, A. W., Brooks, A. G., Whisstock, J. C., Burrows, S. R. *et al.* (2003). A structural basis for the selection of dominant alphabeta T cell receptors in antiviral immunity. *Immunity*, **18**, 53–64.
- Reiser, J. B., Darnault, C., Gregoire, C., Mosser, T., Mazza, G., Kearney, A. *et al.* (2003). CDR3 loop flexibility contributes to the degeneracy of TCR recognition. *Nature Immunol.* **4**, 241–247.
- Garboczi, D. N., Ghosh, P., Utz, U., Fan, Q. R., Biddison, W. E. & Wiley, D. C. (1996). Structure of the complex between human T-cell receptor, viral peptide and HLA-A2. *Nature*, **384**, 134–141.
- Tynan, F. E., Reid, H. H., Kjer-Nielsen, L., Miles, J. J., Wilce, M. C., Kostenko, L. *et al.* (2007). A T cell receptor flattens a bulged antigenic peptide presented by a major histocompatibility complex class I molecule. *Nature Immunol.* **8**, 268–276.
- Chen, J. L., Stewart-Jones, G., Bossi, G., Lissin, N. M., Wooldridge, L., Choi, E. M. *et al.* (2005). Structural and kinetic basis for heightened immunogenicity of T cell vaccines. *J. Expt. Med.* **201**, 1243–1255.
- Lee, J. K., Stewart-Jones, G., Dong, T., Harlos, K., Di Gleria, K., Dorrell, L. *et al.* (2004). T cell cross-reactivity and conformational changes during TCR engagement. *J. Expt. Med.* **200**, 1455–1466.
- Krogsgaard, M., Prado, N., Adams, E. J., He, X. L., Chow, D. C., Wilson, D. B. *et al.* (2003). Evidence that structural rearrangements and/or flexibility during TCR binding can contribute to T cell activation. *Mol. Cell*, **12**, 1367–1378.
- Willcox, B. E., Gao, G. F., Wyer, J. R., Ladbury, J. E., Bell, J. I., Jakobsen, B. K. & van der Merwe, P. A. (1999). TCR binding to peptide-MHC stabilizes a flexible recognition interface. *Immunity*, **10**, 357–365.
- Garcia, K. C., Radu, C. G., Ho, J., Ober, R. J. & Ward, E. S. (2001). Kinetics and thermodynamics of T cell receptor- autoantigen interactions in murine experimental autoimmune encephalomyelitis. *Proc. Natl Acad. Sci. USA*, **98**, 6818–6823.
- Ely, L. K., Beddoe, T., Clements, C. S., Matthews, J. M., Purcell, A. W., Kjer-Nielsen, L. *et al.* (2006). Disparate thermodynamics governing T cell receptor-MHC-I interactions implicate extrinsic factors in guiding MHC restriction. *Proc. Natl Acad. Sci. USA*, **103**, 6641–6646.
- Davis-Harrison, R. L., Armstrong, K. M. & Baker, B. M. (2005). Two different T cell receptors use different thermodynamic strategies to recognize the same peptide/MHC ligand. *J. Mol. Biol.* **346**, 533–550.
- Colf, L. A., Bankovich, A. J., Hanick, N. A., Bowerman, N. A., Jones, L. L., Kranz, D. M. & Garcia, K. C. (2007). How a single T cell receptor recognizes both self and foreign MHC. *Cell*, **129**, 135–146.
- Ellis, J. M., Henson, V., Slack, R., Ng, J., Hartzman, R. J. & Katovich Hurley, C. (2000). Frequencies of HLA-A2 alleles in five U.S. population groups. Predominance Of A*02011 and identification of HLA-A*0231. *Hum. Immunol.* **61**, 334–340.
- Baker, B. M., Turner, R. V., Gagnon, S. J., Wiley, D. C. & Biddison, W. E. (2001). Identification of a crucial energetic footprint on the alpha1 helix of human histocompatibility leukocyte antigen (HLA)-A2 that provides functional interactions for recognition by tax peptide/HLA-A2-specific T cell receptors. *J. Expt. Med.* **193**, 551–562.
- Baxter, T. K., Gagnon, S. J., Davis-Harrison, R. L., Beck, J. C., Binz, A. K., Turner, R. V. *et al.* (2004). Strategic mutations in the class I major histocompatibility complex HLA-A2 independently affect both peptide binding and T cell receptor recognition. *J. Biol. Chem.* **279**, 29175–29184.
- Wang, Z., Turner, R., Baker, B. M. & Biddison, W. E. (2002). MHC allele-specific molecular features determine peptide/HLA-A2 conformations that are recognized by HLA-A2-restricted T cell receptors. *J. Immunol.* **169**, 3146–3154.
- Gagnon, S. J., Borbulevych, O. Y., Davis-Harrison, R. L., Baxter, T. K., Clemens, J. R., Armstrong, K. M. *et al.* (2005). Unraveling a hotspot for TCR recognition on HLA-A2: evidence against the existence of peptide-independent TCR binding determinants. *J. Mol. Biol.* **353**, 556–573.
- Engelhard, V. H. & Benjamin, C. (1982). Isolation and characterization of monoclonal mouse cytotoxic T lymphocytes with specificity for HLA-A,B or -DR alloantigens. *J. Immunol.* **129**, 2621–2629.
- Henderson, R. A., Cox, A. L., Sakaguchi, K., Appella, E., Shabanowitz, J., Hunt, D. F. & Engelhard, V. H. (1993). Direct identification of an endogenous peptide

- recognized by multiple HLA-A2.1-specific cytotoxic T cells. *Proc. Natl Acad. Sci. USA*, **90**, 10275–10279.
27. Buslepp, J., Kerry, S. E., Loftus, D., Frelinger, J. A., Appella, E. & Collins, E. J. (2003). High affinity xenoreactive TCR:MHC interaction recruits CD8 in absence of binding to MHC. *J. Immunol.* **170**, 373–383.
 28. Buslepp, J., Wang, H., Biddison, W. E., Appella, E. & Collins, E. J. (2003). A correlation between TCR Valpha docking on MHC and CD8 dependence: implications for T cell selection. *Immunity*, **19**, 595–606.
 29. Tynan, F. E., Burrows, S. R., Buckle, A. M., Clements, C. S., Borg, N. A., Miles, J. J. *et al.* (2005). T cell receptor recognition of a 'super-bulged' major histocompatibility complex class I-bound peptide. *Nature Immunol.* **6**, 1114–1122.
 30. Clements, C. S., Dunstone, M. A., Macdonald, W. A., McCluskey, J. & Rossjohn, J. (2006). Specificity on a knife-edge: the alphabeta T cell receptor. *Curr. Opin. Struct. Biol.* **16**, 787–795.
 31. Lovell, S. C., Davis, I. W., Arendall, W. B., 3rd, de Bakker, P. I., Word, J. M., Prisant, M. G. *et al.* (2003). Structure validation by C α geometry: phi, psi and C β deviation. *Proteins: Struct. Funct. Genet.* **50**, 437–450.
 32. Madden, D. R. (1995). The three-dimensional structure of peptide-MHC complexes. *Annu. Rev. Immunol.* **13**, 587–622.
 33. Robinson, J., Waller, M. J., Parham, P., de Groot, N., Bontrop, R., Kennedy, L. J. *et al.* (2003). IMGT/HLA and IMGT/MHC: sequence databases for the study of the major histocompatibility complex. *Nucl. Acids Res.* **31**, 311–314.
 34. Ding, Y. H., Smith, K. J., Garboczi, D. N., Utz, U., Biddison, W. E. & Wiley, D. C. (1998). Two human T cell receptors bind in a similar diagonal mode to the HLA-A2/Tax peptide complex using different TCR amino acids. *Immunity*, **8**, 403–411.
 35. Davis-Harrison, R. L., Insaidoo, F. K. & Baker, B. M. (2007). T cell receptor binding transition states and recognition of peptide/MHC. *Biochemistry*, **46**, 1840–1850.
 36. Wu, W., Harley, P. H., Punt, J. A., Sharrow, S. O. & Kears, K. P. (1996). Identification of CD8 as a peanut agglutinin (PNA) receptor molecule on immature thymocytes. *J. Expt. Med.* **184**, 759–764.
 37. Wu, L. C., Tuot, D. S., Lyons, D. S., Garcia, K. C. & Davis, M. M. (2002). Two-step binding mechanism for T-cell receptor recognition of peptide MHC. *Nature*, **418**, 552–556.
 38. James, L. C., Roversi, P. & Tawfik, D. S. (2003). Antibody multispecificity mediated by conformational diversity. *Science*, **299**, 1362–1367.
 39. Chothia, C., Lesk, A. M., Tramontano, A., Levitt, M., Smith-Gill, S. J., Air, G. *et al.* (1989). Conformations of immunoglobulin hypervariable regions. *Nature*, **342**, 877–883.
 40. Chothia, C., Lesk, A. M., Gherardi, E., Tomlinson, I. M., Walter, G., Marks, J. D. *et al.* (1992). Structural repertoire of the human VH segments. *J. Mol. Biol.* **227**, 799–817.
 41. Al-Lazikani, B., Lesk, A. M. & Chothia, C. (1997). Standard conformations for the canonical structures of immunoglobulins. *J. Mol. Biol.* **273**, 927–948.
 42. Morea, V., Tramontano, A., Rustici, M., Chothia, C. & Lesk, A. M. (1998). Conformations of the third hypervariable region in the VH domain of immunoglobulins. *J. Mol. Biol.* **275**, 269–294.
 43. Reiser, J. B., Darnault, C., Guimezanes, A., Gregoire, C., Mosser, T., Schmitt-Verhulst, A. M. *et al.* (2000). Crystal structure of a T cell receptor bound to an allogeneic MHC molecule. *Nature Immunol.* **1**, 291–297.
 44. Borg, N. A., Ely, L. K., Beddoe, T., Macdonald, W. A., Reid, H. H., Clements, C. S. *et al.* (2005). The CDR3 regions of an immunodominant T cell receptor dictate the 'energetic landscape' of peptide-MHC recognition. *Nature Immunol.* **6**, 171–180.
 45. Murshudov, G. N., Vagin, A. A. & Dodson, E. J. (1997). Refinement of macromolecular structures by the maximum-likelihood method. *Acta Crystallog. sect. D*, **53**, 240–255.
 46. Reed, N. S. P. a. R. J. (1996). Improved structure refinement through maximum likelihood. *Acta Crystallog. sect. A*, **52**, 659–668.
 47. Brodsky, F. M., Parham, P., Barnstable, C. J., Crumpton, M. J. & Bodmer, W. F. (1979). Monoclonal antibodies for analysis of the HLA system. *Immunol. Rev.* **47**, 3–61.
 48. Garboczi, D. N., Hung, D. T. & Wiley, D. C. (1992). HLA-A2-peptide complexes: refolding and crystallization of molecules expressed in *Escherichia coli* and complexed with single antigenic peptides. *Proc. Natl Acad. Sci. USA*, **89**, 3429–3433.
 49. Loftus, D. J., Chen, Y., Covell, D. G., Engelhard, V. H. & Appella, E. (1997). Differential contact of disparate class I/peptide complexes as the basis for epitope cross-recognition by a single T cell receptor. *J. Immunol.* **158**, 3651–3658.
 50. Myszka, D. G. & Morton, T. A. (1998). CLAMP: a bio-sensor kinetic data analysis program. *Trends Biochem. Sci.* **23**, 149–150.
 51. Otwinowski, Z. & Minor, W. (1997). Processing of X-ray diffraction data collection in oscillation mode. *Methods Enzymol.* **276**, 307–326.
 52. (1994). The CCP4 suite: programs for protein crystallography. *Acta Crystallog. sect. D*, **50**, 760–763.
 53. Kleywegt, G. J. (1992–2004). Uppsala University, Uppsala, Sweden.
 54. Winn, M. D., Isupov, M. N. & Murshudov, G. N. (2001). Use of TLS parameters to model anisotropic displacements in macromolecular refinement. *Acta Crystallog. sect. D*, **57**, 122–133.
 55. Jones, T. A., Zou, J. Y., Cowan, S. W. & Kjeldgaard (1991). Improved methods for building protein models in electron density maps and the location of errors in these models. *Acta Crystallog. sect. A*, **47**, 110–119.
 56. Lawrence, M. C. & Colman, P. M. (1993). Shape complementarity at protein/protein interfaces. *J. Mol. Biol.* **234**, 946–950.
 57. Baker, B. M. & Murphy, K. P. (1996). Evaluation of linked protonation effects in protein binding reactions using isothermal titration calorimetry. *Biophys. J.* **71**, 2049–2055.

Edited by I. Wilson

(Received 17 April 2007; received in revised form 7 July 2007; accepted 10 July 2007)
Available online 26 July 2007